ACS Macro Letters

Letter

pubs.acs.org/macroletters

Inherently Photohealable and Thermal Shape-Memory Polydisulfide Networks

Brian T. Michal,[†] Colin A. Jaye,[†] Emily J. Spencer,[†,‡] and Stuart J. Rowan*[,†]

[†]Department of Macromolecular Science and Engineering, Case Western Reserve University, 2100 Adelbert Road, Cleveland, Ohio 44106, United States

[‡]Hathaway Brown School, 19600 North Park Boulevard, Shaker Heights, Ohio 44122, United States

Supporting Information

ABSTRACT: Structurally dynamic polydisulfide networks that inherently exhibit both shape-memory and healable properties have been synthesized. These materials are semicrystalline, covalently cross-linked network polymers and as such exhibit thermal shape-memory properties. Upon heating above its melting temperature (T_m) films of the material can be deformed by a force. Subsequent cooling and removal of the force result in the material being "fixed" in this strained temporary shape through a combination of crystallinity and covalent cross-links until it is exposed to temperatures above the T_m at which point it recovers to its remembered processed shape. The incorporation of disulfide bonds, which become dynamic/reversible upon exposure to light or elevated temperatures, into these networks results in them being structurally dynamic upon exposure to the appropriate stimulus. Thus, by activating this disulfide exchange, the network reorganizes, and the material can flow and exhibit healable properties. Furthermore, exposure to light also allows the film's permanent "remembered" shape to be reprogrammed. Shape-memory experiments on these films show high degrees of both fixing and recovery (>95%), and photohealing experiments showed that the films were able to recover from a scratch whose depth is approximately half the thickness of the film. Using a combination of the thermal shape-memory behavior followed by photohealing allows wide scratches to also be efficiently healed.

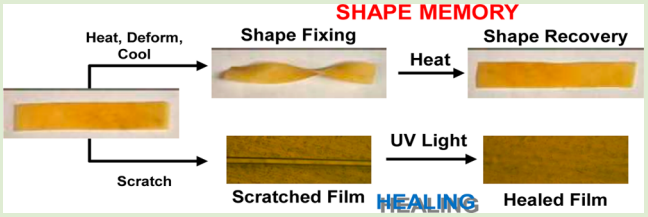

There has been much interest in the design and development of structurally dynamic polymers which act as stimuli-responsive "smart" materials.[1] Such polymers generally include a dynamic bond or interaction within their architecture and thus inherently exhibit the ability to rearrange their structures in response to a stimulus. These dynamic bonds/interactions may be supramolecular in nature (such as hydrogen bonding, π-π stacking, or metal−ligand coordination) or alternatively a dynamic covalent bond.[2,3] Two classes of stimuli-responsive materials that have received significant attention in recent years are shape-memory[4−8] and (self-)healable polymers.[9−14] Shape-memory materials have the ability to convert a fixed temporary shape to a "remembered" (usually the processed) shape upon exposure to an external stimulus. Such materials generally utilize a combination of two or more modes of cross-linking and/or thermal transitions (such as T_g or T_m) to achieve this effect. In a standard shape-memory material, one of the cross-links/thermal transitions will be irreversible under the conditions studied (to remember the processed shaped), and one will be reversible upon exposure to a stimulus (to fix and hold the temporary shape). If covalent cross-linking is used then the remembered state cannot be altered after processing. If a thermal transition is used to remember the permanent shape then the material has the ability to be remodeled after processing.[15,16] In the majority of the materials studied to date a thermal transition is used to fix the material in its strained temporary shape. However, recently it has been shown by a number of groups that reversible cross-linking can be utilized as well. For example, noncovalent interactions, such as hydrogen bonding[17−19] or metal−ligand binding,[20] or dynamic covalent chemistry[21,22] have been shown to allow access to shape-memory materials.

The ability to heal scratches or cracks in a polymer can be achieved irreversibly, either through the release of a polymerizable component stored within microcapsules[23,24] embedded in the material or through the generation of reactive moieties during the deformation process.[25] An alternative approach uses structurally dynamic polymers in which dynamic bonds incorporated into the polymer architecture can be reversibly broken/exchanged. Depending on the nature of the dynamic bond this can happen autonomously or only upon exposure to a stimulus. Inducing this dynamic behavior effectively results in a significant decrease in the molecular weight/viscosity of the polymer, allowing for rapid flow and healing of small cracks and other defects. Thus, most supramolecular polymers exhibit healing behavior.[26−29] Alternatively, there are a number of healable polymers that have been developed which utilize reversible covalent bonds, such as reversible Diels−Alder

Received: June 17, 2013
Accepted: July 17, 2013
Published: July 22, 2013

adducts,[30] olefin metathesis,[31] hydrazone exchange,[32] and transesterification.[33]

The development of materials that combine both shape-memory and (self-)healing is of interest as the shape-memory behavior can be used to aid in the healing process by bringing fractured surfaces into close proximity, allowing them to be more efficiently healed. All the materials reported to date that combine these properties are composite systems which have separate shape-memory and healing components. For example, one technique is to embed shape memory alloy wires into a polymer matrix that also contains embedded capsules of a healing agent[34,35] or solvent.[36] A similar approach is to make a composite material with shape-memory polymer fibers in a polymer matrix which also contains a healing agent.[37] Mather and co-workers recently reported materials with linear poly(ε-caprolactone) (PCL) either blended with cross-linked PCL[38] or as fibers embedded within a shape memory epoxy matrix.[39] In these instances the matrix material provided the shape memory effect for crack closure, and melting and diffusion of the linear PCL provided the healing.

In previous work, we have shown that structurally dynamic polymers (polymers with the ability to reorganize their structure) that contain reversible metal−ligand interactions allow access to films that either have the ability to heal[26] or exhibit shape memory properties[20] upon exposure to light but not both. In these cases the ligand absorbs the light and converts the energy into heat which in turn results in decomplexation of the metal ligand motif. More recently, Weder and co-workers have extended this photothermal healing concept to hydrogen-bonded nanocomposites.[40] While this works well there are some limitations to materials that use such a photothermal conversion process to induce healing. For example, if the material is used as a coating on a substrate that acts as a heat sink (e.g., a metal or glass) then it is difficult for these materials to reach the temperatures that result in efficient healing. The goal of this study was 2-fold, namely, to develop structurally dynamic polymer films that inherently exhibit (1) both shape-memory and healing characteristics and (2) photohealing behavior when used as a coating on a surface that acts as a heat sink. To achieve the latter goal, a dynamic bond was required that undergoes direct photocleavage. Recently the disulfide bond has been shown to be dynamic under a range of stimuli such as heat,[41] light,[42] and pH.[43] Klumperman has shown that heat is effective in healing films of polydisulfide-containing epoxy-based materials,[44] while Anseth and Bowman have shown that light can be used to heal disulfide-containing hydrogels.[45] Related sulfur-containing moieties have also been used to create stimuli-responsive materials.[46] For example, Takahara and Matyjaszewski have reported a material containing thiuram linkages that was shown to be healable using visible light,[47] and Bowman reported a material based on allyl sulfides that demonstrated stress relaxation properties when exposed to UV light.[48]

Thus, a semicrystalline, covalently cross-linked polymer which contains disulfide bonds as an integral component of the network was targeted as a material that would potentially exhibit both photohealing and thermal shape-memory responses as intrinsic properties of the material. The crystalline regions would act as physical dynamic cross-links, which when combined with the covalent cross-links should result in the material exhibiting thermally induced shape-memory properties, while the inclusion of disulfide bonds into the network will result in the material becoming structurally dynamic upon application of light, imparting healable properties to the system.

The targeted material was obtained from three commercially available compounds, 1,6-hexanedithiol (**1**), 1,5-hexadiene (**2**), and the tetrathiol **3** (Scheme 1). To access the required semicrystalline component of the network, the bisthiol oligomer **4** (M_n = 1080 g/mol) was prepared using a photoinduced thiol−ene reaction between **1** and **2** (see Supporting Information, Figure S1). The size of the oligomer/polymer was controlled by simply varying the ratio of the two components. This semicrystalline material exhibited a melting temperature (T_m) of 61.2 °C. The bisthiol oligomer **4** was then polymerized with the tetrathiol cross-linker **3** by oxidative coupling of the thiol moieties using sodium iodide/hydrogen peroxide.[49] The ratio of the two components was controlled to have varying cross-link densities. Three different samples were prepared with their targeted cross-linked density being 4000 (**5**), 8000 (**6**), and 12 000 (**7**) g/mol/cross-link and all exhibited a semicrystalline structure confirmed by WAXD (Figure S2, Supporting Information) with T_m's between 57 and 61 °C (Figure S3, Supporting Information). Dynamic mechanical analysis of these materials (Figure S4, Supporting Information) shows that these films had a T_g of ca. −30 °C.

Initial studies focused on the propensity of these films to be healed by exposure to UV light. To test the effectiveness of such a photohealing process, neat films with an approximate thickness of 300 μm were scored with a razor blade to an approximate depth of 150 μm. The films were then exposed to UV light at a wavelength of 320−390 nm and intensity of 2000 mW/cm^2 for 5 min. During UV exposure the films were placed on a 1 in. thick aluminum block and covered with a glass slide (both of which act as heat sinks). UV light intensity measurements were taken with the same glass slide covering the detector to account for any UV absorption by the slide. The temperature of the specimen during UV exposure was measured using an IR camera and found to not exceed 78 °C during 5 min of exposure (see Supporting Information Figure S5). Figure 1a shows the images of the scratched films before and after UV light exposure. As can be seen, the scratches are

Scheme 1. Synthesis of the Semicrystalline Polydisulfide Network

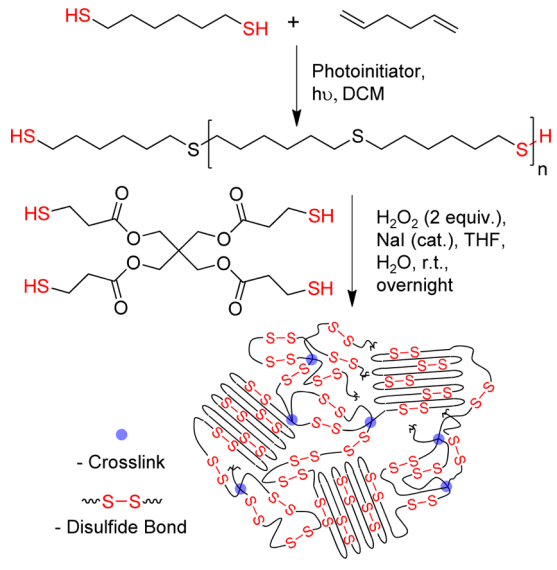

dx.doi.org/10.1021/mz400318m | ACS Macro Lett. 2013, 2, 694−699

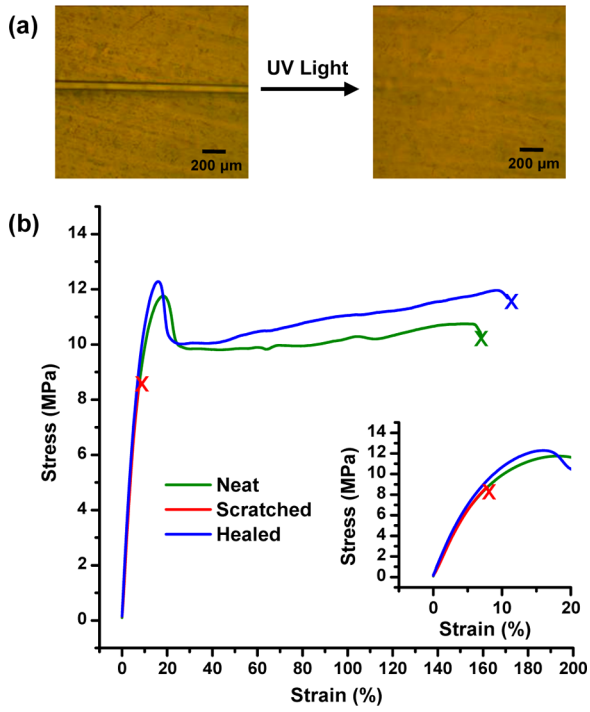

Figure 1. (a) Image showing healing of a scratched film of **6**. The scratched film was exposed to UV light at a wavelength of 320−390 nm and an intensity of 2000 mW/cm^2 for 5 min. (b) Stress−strain curve for representative neat, scratched, and healed samples of **6**.

nearly undetectable after being exposed to these photohealing conditions. To determine the efficiency of the healing process, tensile stress−strain experiments were carried out on dogbone-shaped samples of the films as-processed, scratched, and after exposure to the healing conditions. The as-processed dogbone specimens were scratched perpendicular to the tensile axis at the thinnest region of the neck. Again, the scratch depth was approximately 50% of the film, i.e., 150 μm. The specimens were then healed by exposure to UV light at a wavelength of 320−390 nm and an intensity of 2000 mW/cm^2 for 5 min. Figure 1b shows representative stress−strain plots for the neat, scratched, and healed specimens for **6** (see Supporting Information Figure S6 for corresponding data for **5** and **7**). As expected, the cut in the film dramatically impacts the overall mechanical strength of the film, which breaks easily at the site of the cut. Of course it is important to note the film is not as thick at the cut site. However, for consistency, the stresses for all samples were calculated using the bulk thickness. Upon exposure to the UV light for 5 min the mechanical properties of the film completely recovered (within experimental error). It is interesting to note that exposure to these conditions for 5 min was required to obtain full mechanical recovery (Figure S7, Supporting Information) even though visually the scratch disappeared within a few minutes. For each sample the healing efficiency is calculated as a percent of mechanical toughness recovered upon healing. These data are shown in Table 1 and highlight that within experimental error all three films show complete recovery. It was hypothesized that the relatively large UV intensity required to induce healing was necessary to heat the sample above its melting temperature (T_m ca. 60 °C). To test this, a film of **6** was heated to 80 °C and was shown to fully recover its mechanical properties upon exposure to UV light (320−390 nm) at the much lower intensity of 100 mW/cm^2 for

Table 1. Summary of the Healing Efficiencies and Fixing and Recovery Ratios for the Three Films (Five Samples)

sample	X-link density (g/mol/x-link)	healing efficiency (%)	fixing ratio (%)	recovery ratio (%)
5	4000	103 ± 19	97.7 ± 0.1	98.7 ± 1.9
6	8000	100 ± 22	97.5 ± 0.1	99.6 ± 1.6
7	12000	98 ± 20	99.1 ± 0.1	98.1 ± 6.0

5 min (Figure S8, Supporting Information). It is important to note that heating of the film to 110 °C results in no significant healing of the film.

Having demonstrated the photohealing of these films, the focus turned to their shape-memory properties. These experiments (Figure 2a for **6**) were carried out on films with approximate dimensions of 12 mm × 6 mm × 0.3 mm. After the initial length of the films was recorded, they were heated to 80 °C, and a force of 0.10 N was applied. The films were then cooled to 25 °C and held at this temperature for 1 min. The strain on the film at this point is defined as the maximum strain (ε_m). The force was then removed and the sample allowed to equilibrate for 1 min, after which the unloading strain (ε_u) was measured. The fixing ratio R_f is given as the ratio of the strain

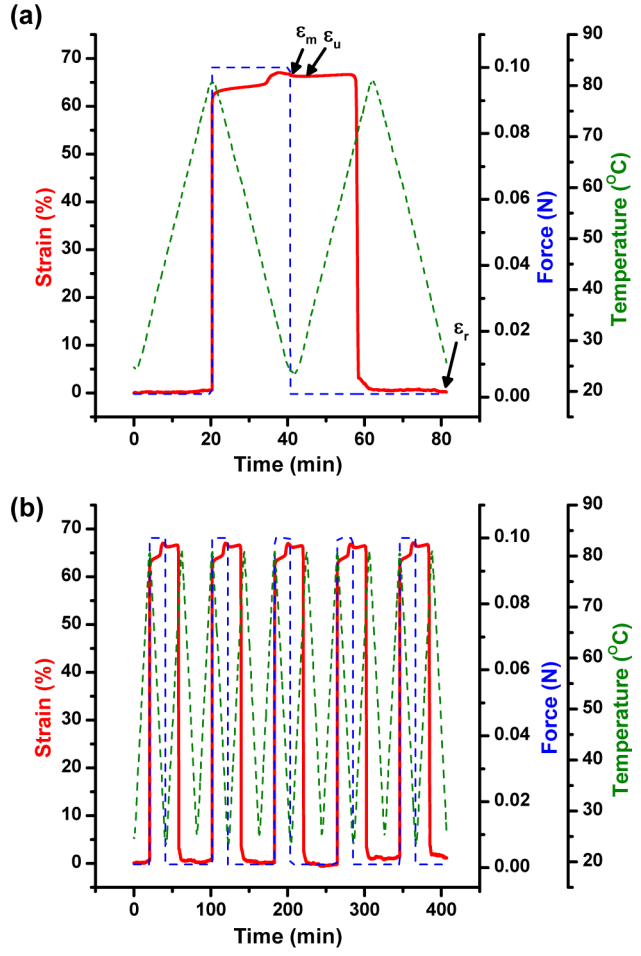

Figure 2. (a) One-way shape-memory cycle for **6**. The film is heated to 80 °C, and a force of 0.10 N is applied to stretch the sample. The sample is then cooled to 25 °C. The force is removed, and the degree of fixing is measured. The sample is then heated to 80 °C and allowed to cool again to 25 °C, and the degree of recovery is measured. (b) Shape memory experiment for **6** showing five cycles.

dx.doi.org/10.1021/mz400318m | ACS Macro Lett. 2013, 2, 694−699

after unloading to the maximum strain ($(\varepsilon_u/\varepsilon_m) \times 100$). To test the recovery of the film, the sample is then heated to 80 °C and held for 1 min before being allowed to cool back to room temperature, and the recovered strain is recorded (ε_r). The recovery ratio (R_r) is given as the percentage of strain recovered ($(\varepsilon_m - \varepsilon_r/\varepsilon_m) \times 100$). Table 1 summarizes both the fixing and recovery ratio for the films, and as can be seen, all three films show excellent shape-memory properties with >95% in both fixing and recovery. Furthermore, these films showed that the fixing and recovery ratios stay consistent over many cycles (Figure 2b, corresponding data for **5** and **7** can be found in Figure S9, Supporting Information). An additional experiment using a force of 0.20 N was also carried out on **6** to examine the shape-memory effect of these films at higher strain (Figure S10, Supporting Information). The fixing and recovery rates at these higher strains (>100%) were also >95%.

Most shape-memory materials use permanent covalent cross-links to define the recoverable shape. These are usually set during a curing process, at which point the permanent shape of the material is determined. As these materials can become structurally dynamic upon exposure to an appropriate stimulus, it should be possible to "reprogram" the remembered shape of this film by simply exposing the film to light while remolding it into the new desired shape. Figure 3 shows an example of the reprogramming ability of this material. In the top left image the material starts as a flat film. It exhibits standard shape-memory behavior by heating to 80 °C, being deformed (by twisting), and then cooling to give it a fixed helical shape. Upon reheating to 80 °C, the material recovers to the flat film. However, if the material is deformed by twisting while being exposed to UV light, the material's recoverable shape is reprogrammed to the helical shape, as shown in the images on the right-hand side of Figure 3. Namely, the material can be heated, deformed, and cooled to give it a temporary fixed flat shape which recovers to the helical twisted form upon reheating. Of course, as the disulfide bond is also dynamic at higher temperature we can also reprogram the permanent shape by simply melt processing at 180 °C (see Supporting Information Figure S11 and Supporting Videos).

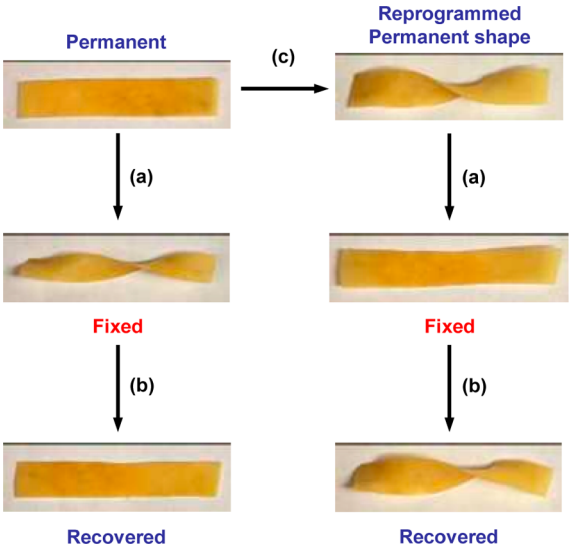

Figure 3. Pictures showing the reprogrammable shape memory properties of **6**. The specimen is pressed as a flat film and then (a) heated to 80 °C while being held in a helical shape. (b) The film is then heated to 80 °C and allowed to recover to the permanent shape. (c) The permanent shape of the film can be photoreprogrammed by holding it in the helical shape while exposing it to UV light.

Finally, the ability to combine both the thermal shape-memory and photohealing capabilities of the material to heal relatively wide scratch damage was examined. This was accomplished by prestretching the material above its melting temperature to create a set strain. Figure 4a shows a sample of **6** that was prestrained to 100% and then damaged with an approximately 200 μm wide gouge, created by repeated slicing with a razor blade. When the material is heated above the melting temperature of the crystalline regions, the shape recovery is activated, and the material compresses/recovers. This results in the damaged surfaces being moved into closer proximity, reducing the width of the defect to that similar to a normally scratched sample. From there, the material can then be healed by exposure to UV light at a wavelength of 320–390 nm and an intensity of 2000 mW/cm^2 for 5 min as shown previously.

Figure 4b shows tensile stress strain data for a sample of **6** in the neat, prestrained, scratched, sealed, and healed conditions. The prestrained specimen (strained to 100% above its T_m and cooled under this strain) shows an increase in the ultimate

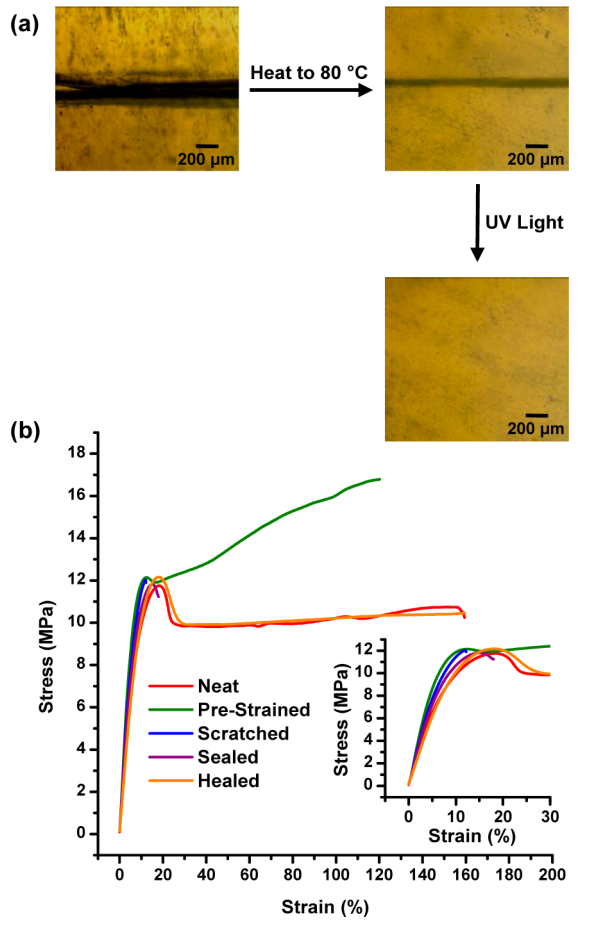

Figure 4. (a) Sample of **6** prestrained to 100% and then given a deep gouge by repeated cutting with a razor blade. Heating to 80 °C allows for shape recovery which forces the two damaged surfaces into closer proximity. Healing can then be carried out exposing the sample to UV light at an intensity of 2000 mW/cm^2 and wavelength of 320–390 nm for 5 min. (b) Stress–strain curve for representative neat, prestrained, scratched, sealed, and healed samples of **6**.

dx.doi.org/10.1021/mz400318m | ACS Macro Lett. 2013, 2, 694–699

tensile stress of the material and a decrease in its ductility. Scratching the prestrained material to a depth of approximately half of the film thickness and a width of approximately 200 μm results in a near complete loss of the mechanical properties. The scratched material is then "sealed" by immersing in a water bath at 80 °C for 10 s which allows the material to recover to its original length and reduce the width of the scratch. However, no recovery of mechanical properties occurs during this step since the scratch still remains in the material. Finally, the sample is exposed to UV light at a wavelength of 320−390 nm and an intensity of 2000 mW/cm^2 for 5 min resulting in complete recovery of the mechanical properties. It is worthy to note that attempting to heal a prestrained sample without first heat treating to allow for shape recovery resulted in significant warping of the material as uneven heating during the photohealing process resulted in nonunifiorm relaxation of the network.

In summary, semicrystalline, covalently cross-linked networks that contain disulfide bonds have been shown to form films that intrinsically exhibit both thermal (at 80 °C) shape-memory and photohealable behavior. Using these properties in combination imparts on the film the ability to heal relatively large scratches/deformations. Furthermore, these cross-linked films also have the ability to reconfigure/reprogram their permanent, "remembered" shape by simple exposure to light or relatively high (ca. 180 °C) temperature.

■ ASSOCIATED CONTENT

Supporting Information

Experimental section describing the synthesis of the bisthiol oligomers and the disulfide networks. Differential scanning calorimetry curves and wide-angle X-ray diffraction patterns for all samples, recovery of mechanical properties as a function of healing time, thermal imaging of samples during healing, healing experiment maintaining a sample at elevated temperature, stress−strain curves for neat, healed, and scratched specimens of **5** and **7**, five-cycle shape-memory experiments for **5** and **7**, DMA temperature sweeps for all samples, and shape memory experiments for **6** with 0.20 N applied force. This material is available free of charge via the Internet at http://pubs.acs.org.

■ AUTHOR INFORMATION

Corresponding Author

*E-mail: stuart.rowan@case.edu.

Notes

The authors declare no competing financial interest.

■ ACKNOWLEDGMENTS

The authors gratefully acknowledge financial support from the National Aeronautics and Space Administration (Grant no. NNX11AN50H) and Army Research Office (Grant no. W911NF-12-1-0339).

■ REFERENCES

(1) (a) Wojtecki, R. J.; Meador, M. A.; Rowan, S. J. *Nat. Mater.* **2011**, *10*, 14−27. (b) Bowman, C. N.; Kloxin, C. J. *Angew. Chem., Int. Ed.* **2012**, *51*, 4272−4274.
(2) Rowan, S. J.; Cantrill, S. J.; Cousins, G. R. L.; Sanders, J. K. M.; Stoddart, J. F. *Angew. Chem., Int. Ed.* **2002**, *41*, 899−952.
(3) Maeda, T.; Otsuka, H.; Takahara, A. *Adv. Polym. Sci.* **2009**, *34*, 581.
(4) Xie, T. *Polymer* **2011**, *52*, 4985−5000.
(5) Zhao, Q.; Behl, M.; Lendlein, A. *Soft Matter* **2013**, *9*, 1744−1755.
(6) Hu, J.; Zhu, Y.; Huang, H.; Lu, J. *Prog. Polym. Sci.* **2012**, *37*, 1720−1763.
(7) Huang, W. M.; Zhao, Y.; Wang, C. C.; Ding, Z.; Purnawali, H.; Tang, C.; Zhang, J. L. *J. Polym. Res.* **2012**, *19*, 9952−9985.
(8) Hao, J.; Weiss, R. A. *ACS Macro Lett.* **2013**, *2*, 86−89.
(9) Murphy, E. B.; Wudl, F. *Prog. Polym. Sci.* **2010**, *35*, 223−251.
(10) Burattini, S.; Greenland, B. W.; Chappell, D.; Colquhoun, H. M.; Hayes, W. *Chem. Soc. Rev.* **2010**, *39*, 1973−1985.
(11) Syrett, J. A.; Becer, C. R.; Haddleton, D. M. *Polym. Chem.* **2010**, *1*, 978−987.
(12) Wool, R. P. *Soft Matter* **2008**, *4*, 400−418.
(13) Seiffert, S.; Sprakel, J. *Chem. Soc. Rev.* **2012**, *41*, 909−930.
(14) Fiore, G. L.; Rowan, S. J.; Weder, C. *Chem. Soc. Rev.* **2013**, DOI: 10.1039/C3CS35471G.
(15) Fei, P.; Cavicchi, K. A. *ACS Appl. Mater. Interfaces* **2010**, *2*, 2797−2803.
(16) Luo, X. F.; Mather, P. T. *Adv. Funct. Mater.* **2010**, *20*, 2649−2656.
(17) Li, J.; Viveros, J. A.; Wrue, M. H.; Anthamatten, M. *Adv. Mater.* **2007**, *19*, 2851−2855.
(18) Kushner, A. M.; Vossler, L.; Williams, G. A.; Guan, Z. *J. Am. Chem. Soc.* **2009**, *131*, 8766−8768.
(19) Mendez, J.; Annamalai, P. K.; Eichhorn, S. J.; Rusli, R.; Rowan, S. J.; Foster, E. J.; Weder, C. *Macromolecules* **2011**, *44*, 6827−6835.
(20) Kumpfer, J. R.; Rowan, S. J. *J. Am. Chem. Soc.* **2011**, *133*, 12866−12874.
(21) Lendlein, A.; Jiang, H.; Junger, O.; Langer, R. *Nature* **2005**, *434*, 879−882.
(22) Aoki, D.; Teramoto, Y.; Nishio, Y. *Biomacromolecules* **2007**, *8*, 3749−3757.
(23) White, S. R.; Sottos, N. R.; Geubelle, P. H.; Moore, J. S.; Kessler, M. R.; Sriram, S. R.; Brown, E. N.; Viswanathan, N. *Nature* **2001**, *409*, 794−797.
(24) Na, X.-M; Gao, F.; Zhang, L.-Y.; Su, Z.-G.; Ma, G.-H. *ACS Macro Lett.* **2012**, *1*, 697−700.
(25) (a) Ghosh, B.; Urban, M. W. *Science* **2009**, *323*, 1458−1460. (b) Jakobs, R. T. M.; Ma, S.; Sijbesma, R. P. *ACS Macro Lett.* **2013**, *2*, 613−616.
(26) Burnworth, M.; Tang, L.; Kumpfer, J. R.; Duncan, A. J.; Beyer, F. L.; Fiore, G. L.; Rowan, S. J.; Weder, C. *Nature* **2011**, *472*, 334−338.
(27) Cordier, P.; Tournilhac, F.; Soulie-Ziakovic, C.; Leibler, L. *Nature* **2008**, *451*, 977−980.
(28) Chen, Y.; Kushner, A. M.; Williams, G. A.; Guan, Z. *Nature Chem.* **2012**, *4*, 467−472.
(29) Zhang, H.; Xia, H.; Zhao, Y. *ACS Macro Lett.* **2012**, *1*, 1233−1236.
(30) (a) Chen, X.; Dam, M. A.; Ono, K.; Mal, A.; Shen, H.; Nutt, S. R.; Sheran, K.; Wudl, F. *Science* **2002**, *295*, 1698−1702. (b) Imbesi, P. M.; Fidge, C.; Raymond, J. E.; Cauet, S. I.; Wooley, K. L. *ACS Macro Lett.* **2012**, *1*, 473−477. (c) Thongsomboon, W.; Sherwood, M.; Arellano, N.; Nelson, A. *ACS Macro Lett.* **2013**, *1*, 19−22.
(31) (a) Lu, Y.-X.; Guan, Z. *J. Am. Chem. Soc.* **2012**, *134*, 14226−14231.
(32) Deng, G.; Tang, C.; Li, F.; Jiang, H.; Chen, Y. *Macromolecules* **2010**, *43*, 1191−1194.
(33) Capelot, M.; Montarnal, D.; Tournilhac, F.; Leibler, L. *J. Am. Chem. Soc.* **2012**, *134*, 7664−7667.
(34) Kirkby, E. L.; Rule, J. D.; Michaud, V. J.; Sottos, N. R.; White, S. R.; Manson, J. A. E. *Adv. Funct. Mater.* **2008**, *18*, 2253−2260.
(35) Kirkby, E. L.; Michaud, V. J.; Manson, J. A. E.; Sottos, N. R.; White, S. R. *Polymer* **2009**, *50*, 5533−5538.
(36) Neuser, S.; Michaud, V.; White, S. R. *Polymer* **2012**, *53*, 370−378.
(37) Li, G.; Meng, H.; Hu, J. *J. R. Soc. Interface* **2012**, *9*, 3279−3287.
(38) Rodriguez, E. D.; Luo, X.; Mather, P. T. *ACS Appl. Mater. Interfaces* **2011**, *3*, 152−161.
(39) Luo, X.; Mather, P. T. *ACS Macro Lett.* **2013**, *2*, 152−156.

(40) Biyani, M. V.; Foster, E. J.; Weder, C. *ACS Macro Lett.* **2013**, *2*, 236−240.
(41) Yoon, J. A.; Kamada, J.; Koynov, K.; Mohin, J.; Nicolay, R.; Zhang, Y.; Balazs, A. C.; Kowalewski, T.; Matyjaszewski, K. *Macromolecules* **2012**, *45*, 142−149.
(42) Otsuka, H.; Nagano, S.; Kobashi, Y.; Maeda, T.; Takahara, A. *Chem. Commun.* **2010**, *46*, 1150−1152.
(43) Deng, G.; Li, F.; Yu, H.; Liu, F.; Liu, C.; Sun, W.; Jiang, H.; Chen, Y. *ACS Macro Lett.* **2012**, *1*, 275−279.
(44) Canadell, J.; Goossens, H.; Klumperman, B. *Macromolecules* **2011**, *44*, 2536−2541.
(45) Fairbanks, B. D.; Singh, S. P.; Bowman, C. N.; Anseth, K. S. *Macromolecules* **2011**, *44*, 2444−2450.
(46) Amamoto, Y.; Otsuka, H.; Takahara, A.; Matyjaszewski, K. *ACS Macro Lett.* **2012**, *1*, 478−481.
(47) Amamoto, Y.; Otsuka, H.; Takahara, A.; Matyjaszewski, K. *Adv. Mater.* **2012**, *24*, 3975−3980.
(48) Scott, T. F.; Schneider, A. D.; Cook, W. D.; Bowman, C. N. *Science* **2005**, *308*, 1615−1617.
(49) Kirihara, M.; Asai, Y.; Ogawa, S.; Noguchi, T.; Hatano, A.; Hirai, Y. *Synthesis* **2007**, *No. 21*, 3286.